Zeolites

DOI: 10.1002/anie.201104462

Detailed Reaction Paths for Zeolite Dealumination and Desilication From Density Functional Calculations**

Sami Malola, Stian Svelle, Francesca Lønstad Bleken, and Ole Swang*

Zeolites, which are crystalline microporous aluminosilicates, have found widespread industrial application, not least because of their combination of porosity and acidity; the latter arises from the substitution of silicon atoms by aluminum/proton pairs. Zeolites may be partially hydrolyzed by steaming, thereby decreasing their crystallinity, but in some cases improving their efficiency as catalysts as both pore structure and acidity are modified. Zeolite Y, the catalytic cracking catalyst used to produce one-third of all gasoline fuel, is always steamed. Recently, treatment with dilute alkali solution has emerged as an efficient means of introducing mesoporosity, leading to enhanced catalyst performance.[1] Moreover, zeolite catalysts are exposed to steam during regeneration by the oxidation of carbon deposits, which leads to a slow degradation process referred to as irreversible deactivation. Both kinds of tetrahedral atoms, Al and Si, may be hydrolyzed, and both cases have been studied in the literature.[2–4] The full hydrolysis of a tetrahedral atom leaves a moiety called a hydrogarnet defect or silanol nest, in which four hydroxy groups mingle in hydrogen-bonded fashion in the void left by the tetrahdral atom.[5] Along with the Brønsted acid sites, zeolites may contain Lewis acid sites consisting of hydrated Al species residing within the pores. Such extra-framework Al (EFAl) compounds have been studied extensively[6] and show significant mobility.[7] Atom-scale modeling has become an important complement to experimental techniques in many areas of chemistry and solid state science, and some aspects pertaining to the removal of zeolite tetrahedral atoms in steam have been investigated. Sokol et al.[8] studied silanol nests and the vicinal disilanol species (the latter containing five-coordinate Si) using atom-scale modeling. Furthermore, they investigated the dehydration/dehydrogenation (with peroxide formation) of silanol nests, and suggest possible mechanisms for healing the defect. Pascale et al.[9] computed the formation energy of a silanol nest with respect to orthosilicic acid (H_4SiO_4) and reported the structure of nests from different computational approaches. Lisboa et al.,[10] using semiempirical calculations and cluster models, studied a number of reaction intermediates for dealumination of a zeolite. Activation and reaction energies were not reported, as the chosen method does not afford quantitative energies. Thus, very little fundamental insight concerning the hydrolysis reaction chain itself is available, despite widespread application of steaming and the high relevance to understanding the irreversible deactivation of zeolite catalysts. Herein, we present unprecedented insights for tetrahedral-atom extraction by reaction with steam, including first-principles DFT reaction and activation energies for all steps of dealumination and desilication of the zeolite.

To address these complex processes in a computationally feasible manner, we have chosen as a natural first approach in this initial work, to add water molecules sequentially. Thus, dealumination is a series of hydration reactions, where at least three water molecules are needed to form a silanol nest and detach Al in the form of $Al(OH)_3$. Adsorption of a fourth water molecule creates a more stable $Al(OH)_3(H_2O)$ EFAl compound (Figure 1). To create a silanol nest via the analogous process of desilication, at least four hydration reactions are needed, and the extra-framework compound after desilication is tetrahedral $Si(OH)_4$ (Figure 1). Adding only one water molecule at a time is clearly an approximation to the experimental situation in which a significant steady-state vapor pressure exists in the pore system. Moreover, we do not follow the hydration process beyond the formation of extra framework species that are expected to display mobility within the pores (see below). Finally, temperature effects are not explicitly accounted for.

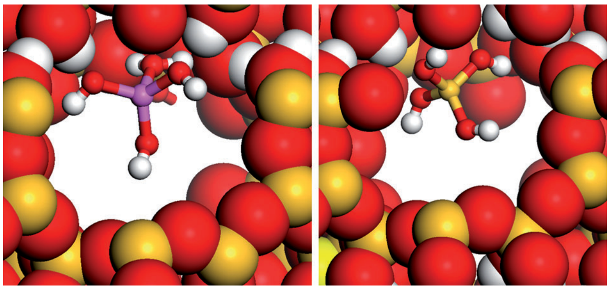

Figure 1. Final configurations after dealumination (left) and desilication (right). O red, Si yellow, H white, Al purple.

We consider two different initial conditions in our analyses—the reactant energy for each step can either be

---

[*] Dr. S. Malola, Prof. Dr. S. Svelle, Dr. F. L. Bleken, Dr. O. Swang
inGAP Center for Research-Based Innovation
Department of Chemistry, University of Oslo
P. O. Box 1033 Blindern, 0315 Oslo (Norway)
E-mail: ole.swang@sintef.no
Homepage: http://www.ingap.uio.no
Dr. O. Swang
SINTEF Materials and Chemistry, Department of Process Chemistry
P. O. Box 124 Blindern, 0314 Oslo (Norway)

[**] Thanks are due to the Norwegian High Performance Computing program (http://www.notur.no) for a generous grant of computing resources. S.M. acknowledges a postdoctoral fellowship from the Research Council of Norway under the KOSK program.

Supporting information for this article is available on the WWW under http://dx.doi.org/10.1002/anie.201104462.

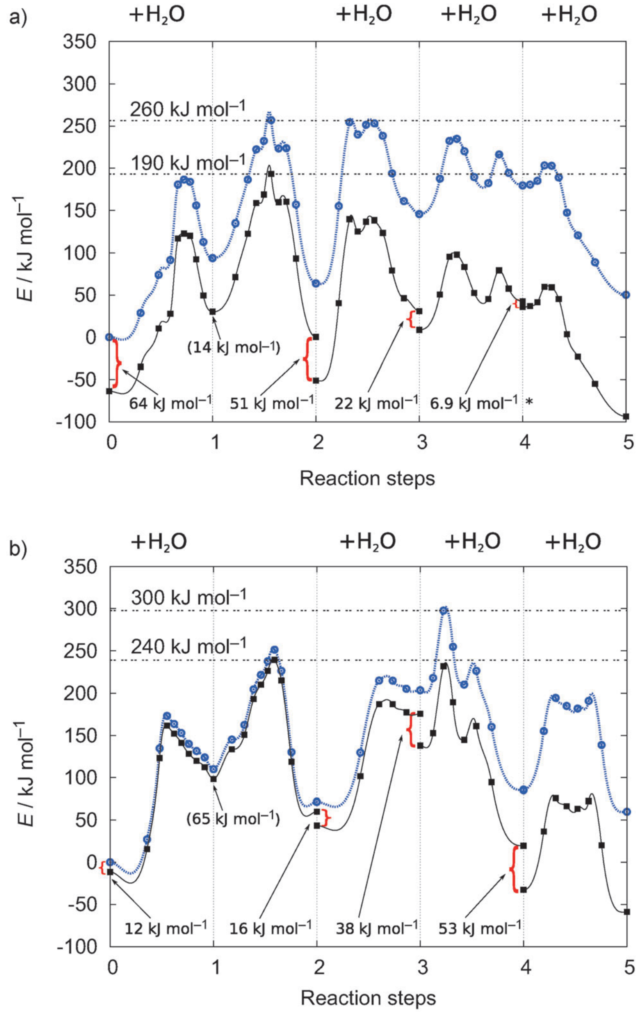

Figure 2. Reaction paths for a) dealumination and b) desilication combined from five different NEB paths. Black lines: approach A, considering initially isolated water molecules; purple lines: approach B, considering initially adsorbed water molecules. Effective barriers for both approaches are labeled in the upper left corner. Adsorption energies of the water molecules are seen as discontinuous jumps for each intermediate state. For state 1 in both processes, adsorption energies (shown in parentheses) are calculated only for comparison; water is not added at state 1.

calculated for a water molecule in vacuo, or a water molecule adsorbed on site, resulting in different relative energies for each step (Figure 2). Approach A (black lines in Figure 2) take the adsorption of each water molecule explicitly into account during the process. Approach B (purple lines) omits the energy gain by water adsorption at each step and thus to a larger degree resembles a system in which water molecules are adsorbed or saturated on the surface of the zeolite before initiation of the hydrolysis reactions. Although we do not go past four added water molecules, the two abovementioned approaches may be regarded as approximate upper and lower limits for the reaction energies.

A reaction proposal is shown in Figure 3. The reaction steps for dealumination are:

0→1: First hydration, including formation of a vicinal disilanol defect;

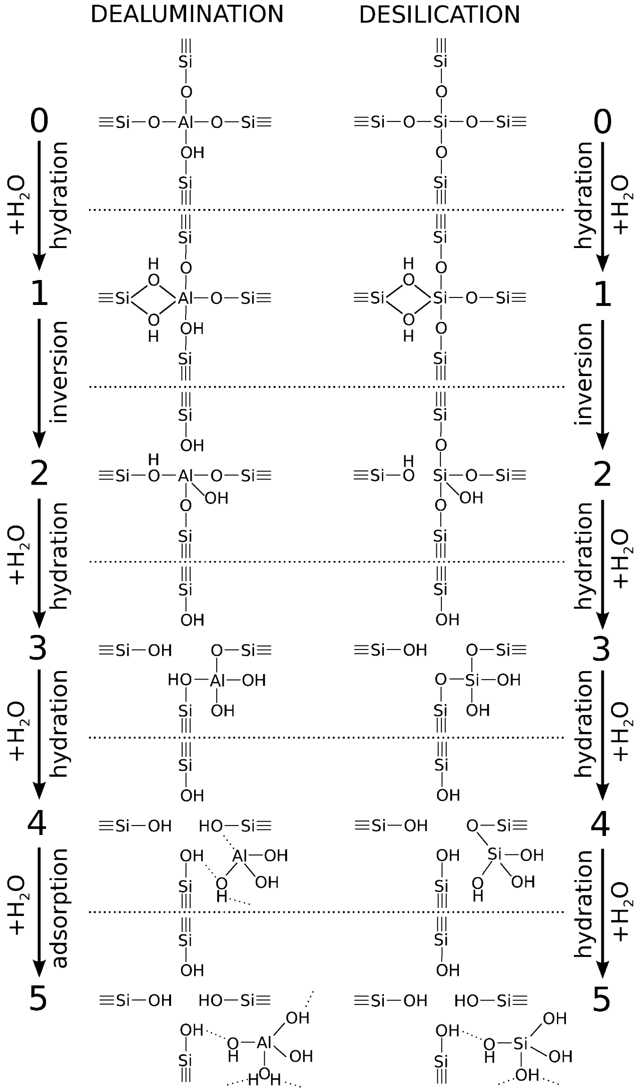

Figure 3. Reaction steps with intermediate configurations shown for dealumination (left) and for desilication (right); —— covalent bonds; •••• hydrogen bonds. Based on our observations, tetrahedral atoms are not at their original sites after step 2→3.

1→2: Inversion of an OH group and reorientation of the bonds;

2→3: Second hydration, giving four loosely bound OH groups as a product: two bound to the Si and two to the Al;

3→4: Third hydration, giving partially bonded $Al(OH)_3$ as a product;

4→5: Adsorption of the fourth H_2O molecule, thereby detaching the final $Al(OH)_3(H_2O)$ EFAl compound.

The final step (4→5) is replaced by a fourth hydration in the case of desilication, giving extra-framework $Si(OH)_4$. Effective activation energies can be estimated from the highest energies of the curves in Figure 2. For the total dealumination process, the barrier is 190 kJ mol^{-1} with approach A and 260 kJ mol^{-1} with approach B. For the desilication, the energy barrier is 40–50 kJ mol^{-1} larger:

240 kJ mol^{-1} with approach A and 300 kJ mol^{-1} with approach B. This means that Al is substantially less stable as a framework species relative to Si in a steam atmosphere. Gratifyingly, this is also the experimental observation. For the reverse processes, barriers are 290 kJ mol^{-1} and 200 kJ mol^{-1} for alumination and 300 kJ mol^{-1} and 240 kJ mol^{-1} for silication with approaches A and B, respectively. For the total hydrolysis processes, the effective barriers (rate-determining steps) are defined by OH inversion, step 1→2, for dealumination and by OH inversion together with the third hydration reaction, step 3→4, for desilication.

We now turn to the final states. After the third hydration at step (3→4), $Al(OH)_3$ is bound to the framework with two hydrogen bonds of lengths 1.37 and 1.88 Å, and with one weak Al-OH-Si bridge including a 2.02 Å Al–O bond. The final EFAl product of the dealumination, $Al(OH)_3(H_2O)$, is free from such bridges and bound to the framework with four hydrogen bonds (Figure 3) with lengths 1.55, 1.60, 1.70, and 1.97 Å and with an energy of 145 kJ mol^{-1}. Thus, the final hydration, coordinating H_2O to Al, is necessary for removing the EFAl species from the framework. For desilication, the adsorption energy of the final extra-framework molecule $Si(OH)_4$ is much smaller (77 kJ mol^{-1}), and the compound is bound to the framework with three weak hydrogen bonds about 1.8 Å long. These observations, that is, weak hydrogen bonding leading to moderate adsorption energies for the final extra-framework species, suggest substantial mobility, especially at high temperature in a steam atmosphere such as during steaming or regeneration.

In experimental practice, dealumination is often seen as a change in coordination of aluminum, most often using solid-state ^{27}Al NMR spectroscopy,[11–15] but IR spectroscopy,[16] XANES,[17] XPS,[18] and TPD-MS[19] have been employed. Several experimental studies suggest that steaming leads to the formation of octahedrally coordinated aluminum, identifying this as EFAl species. However, experimental evidence for three-coordinate aluminum in zeolites after steaming has also been reported.[15–18] Perusal of Figure 3 reveals some deviations from fourfold coordination during the process: Species 1 is five-coordinate, whereas species 4 might be interpreted as being three-coordinate (for dealumination only). However, most of the structures proposed for three-coordinate aluminum are less hydrolyzed and rather the result of dehydroxylation.[17] At this point, it should be noted that the calculations presented herein are minimum estimates for the coordination of aluminum owing to the sequential mode of water addition mentioned above. We anticipate that addition of further water molecules to species 5 (Figure 3) would straightforwardly lead to the formation of a six-coordinate octahedral EFAl species, which has been studied in isolated form by others.[6,7] Based on these considerations, we identify the investigations of the effects of allowing water clusters, rather than single water molecules, to reside within the zeolite pores during dealumination and desilication to be a high priority issue for further work.

In conclusion, our results support the experimental observations: both Al and Si may be removed by steam, but dealumination is the least activated of the two. Several systematic differences favor dealumination over desilication. Effective barriers are 40–50 kJ mol^{-1} lower, and adsorption of the water molecules involved in hydration reactions is on average stronger. Intermediate configurations are relatively more stable for dealumination, compensating the slightly higher activation energies of the intermediate reaction steps compared to desilication. The differences between Si and Al may be explained by the well-known coordination flexibility of the latter and the higher polarity of the Al-induced Brønsted site. In a recent multitechnique study of dealumination of zeolite Y, Agostini et al.[20] surprisingly found that most of the framework Al is removed during cooling, concurrent to repopulation of the framework by water. Our results might explain this finding, as the effective energy barrier for dealumination is close to the barrier needed to form the simplest vicinal disilanol defects, and all subsequent hydration steps are rapid. Finally, the present study provides a reasonable mechanism for the mobility of tetrahedral atoms. Understanding the long-term deactivation of silicoaluminophosphates by formation of framework Si islands, leading to permanent loss of Brønsted acid sites, is an important issue.[21] We suggest that such processes may occur by tetrahedral-atom hydrolysis, migration, and reinsertion into another silanol nest, which are known to be abundant. Further work to elucidate the effects of local tetrahedral-atom environment and basicity on the framework extraction process, the influence of water clusters, as well as other possible migration mechanisms is in progress in our laboratories.

Experimental Section

Periodic calculations based on the pseudopotential approximation and the Perdew–Burke–Ernzerhof (PBE) density functional[22] were carried out with the QUANTUM-ESPRESSO program.[23] The nudged elastic band (NEB) approach was used for tracing reaction paths, thereby localizing transition states. The 36-atom unit cell of chabazite (CHA) was used for the production calculations. Some results were re-calculated with larger unit cells to evaluate the effects of periodicity. To evaluate the reliability of the PBE functional, selected relative energies were calculated with the B3LYP hybrid functional[24] using the CASTEP code.[25] The choice of functional or unit cell size does not influence the conclusions presented herein. Further details can be found in the Supporting Information.

Received: June 28, 2011
Revised: October 4, 2011

Keywords: density functional calculations · reaction mechanisms · zeolites

---

[1] J. C. Groen, L. A. A. Peffer, J. A. Moulijn, J. Pérez-Ramírez, *J. Mater. Chem.* **2006**, *16*, 2121.
[2] H. K. Beyer, *Mol. Sieves* **2002**, *3*, 203.
[3] R. M. Ravenelle, F. Schussler, A. D'Amico, N. Danalina, J. van Bokhoven, J. A. Lercher, C. W. Jones, C. Sievers, *J. Phys. Chem. C* **2010**, *114*, 19582.
[4] B. Gil, Ł. Mokrzycki, B. Sulikowski, Z. Olejniczak, S. Walas, *Catal. Today* **2010**, *152*, 24; J. C. Groen, J. C. Jansen, J. A. Moulijn, J. Pérez-Ramirez, *J. Phys. Chem. B* **2004**, *108*, 13062, and references therein.

[5] S. Bordiga, I. Roggero, P. Ugliengo, A. Zecchina, V. Bolis, G. Artioli, R. Buzzoni, G. Marra, F. Rivetti, G. Spanò, C. Lamberti, *J. Chem. Soc. Dalton Trans.* **2000**, 3921; S. Bordiga, P. Ugliengo, A. Damin, C. Lamberti, G. Spoto, A. Zecchina, G. Spanò, R. Buzzoni, L. Dalloro, F. Rivetti, *Top. Catal.* **2001**, *15*, 43.

[6] S. Li, A. Zheng, Y. Su, H. Zhang, L. Chen, J, Yang, C. Ye, F. Deng, *J. Am. Chem. Soc.* **2007**, *129*, 11161; Z. Wu, A. Zheng, Q. Wang, L. Chen, J.-P. Amoreux, F. Deng, *Angew. Chem.* **2010**, *122*, 8839; *Angew. Chem. Int. Ed.* **2010**, *49*, 8657; D. L. Bhering, A. Ramirez-Solis, C. J. A. Mota, *J. Phys. Chem. B* **2003**, *107*, 4342; S. Li, A. Zheng, Y. Su, H. Fang, W. Shen, Z. Yu, L. Chen, F. Deng, *Phys. Chem. Chem. Phys.* **2010**, *12*, 3895.

[7] L. Benco, T. Demuth, J. Hafner, F. Hutschka, H. Toulhoat, *J. Catal.* **2002**, *209*, 480.

[8] A. Sokol, C. R. A. Catlow, J. M. Garcés, A. Kuperman, *J. Phys. Chem. B* **1998**, *102*, 10647; A. Sokol, C. R. A. Catlow, J. M. Garcés, A. Kuperman, *Adv. Mater.* **2000**, *12*, 1801; A. Sokol, C. R. A. Catlow, J. M. Garcés, A. Kuperman, *J. Phys. Chem. B* **2002**, *106*, 6163; A. Sokol, C. R. A. Catlow, J. M. Garcés, A. Kuperman, *J. Phys. Chem. B* **2002**, *106*, 6163; A. Sokol, C. R. A. Catlow, J. M. Garcés, A. Kuperman, *J. Phys. Condens. Matter* **2004**, *16*, S2781.

[9] F. Pascale, P. Ugliengo, B. Civalleri, R. Orlando, P. D'Arco, R. Dovesi, *J. Chem. Phys.* **2002**, *117*, 5337.

[10] O. Lisboa, M. Sánchez, F. Ruette, *J. Mol. Catal. A* **2008**, *294*, 93.

[11] B. H. Wouters, T.-H. Chen, P. J. Grobet, *J. Am. Chem. Soc.* **1998**, *120*, 11419.

[12] A. Omegna, J. A. van Bokhoven, R. Prins, *J. Phys. Chem. B* **2003**, *107*, 8854.

[13] J. Jiao, J. Kanelloupoulos, S. S. Ray, H. Foerster, D. Freude, M. Hunger, *Phys. Chem. Chem. Phys.* **2005**, *7*, 3221.

[14] E. Bourgeat-Lami, P. Massiani, F. di Renzo, P. Espiau, F. Fajula, T. des Courières, *Appl. Catal.* **1991**, *72*, 139.

[15] J. Jiao, S. Altwasser, W. Wang, J. Weitkamp, M. Hunger, *J. Phys. Chem. B* **2004**, *108*, 14305.

[16] A. Zecchina, S. Bordiga, G. Spoto, D. Scarano, G. Petrini, G. Leofanti, M. Padovan, C. Otero Areàn, *J. Chem. Soc. Faraday Trans.* **1992**, *88*, 2959.

[17] J. A. van Bokhoven, A. M. J. van der Eerden, D. C. Koningsberger, *J. Am. Chem. Soc.* **2003**, *125*, 7435.

[18] F. Collignon, P. A. Jacobs, P. Grobet, G. Poncelet, *J. Phys. Chem. B* **2001**, *105*, 6812.

[19] M. J. Nash, A. M. Shough, D. W. Fickel, D. J. Doren, R. F. Lobo, *J. Am. Chem. Soc.* **2008**, *130*, 2460.

[20] G. Agostini, C. Lamberti, L. Palin, M. Milanesio, N. Danilina, B. Xu, M. Janousch, J. A. van Bokhoven, *J. Am. Chem. Soc.* **2010**, *132*, 667.

[21] G. Sastre, D. W. Lewis, C. R. A. Catlow, *J. Phys. Chem.* **1996**, *100*, 6722.

[22] J. P. Perdew, K. Burke, M. Ernzerhof, *Phys. Rev. Lett.* **1996**, *77*, 3865.

[23] P. Giannozzi, S. Baroni, N. Bonini, M. Calandra, R. Car, C. Cavazzoni, D. Ceresoli, G. L. Chiarotti, M. Cococcioni, I. Dabo, A. Dal Corso, S. de Gironcoli, S. Fabris, G. Fratesi, R. Gebauer, U. Gerstmann, C. Gougoussis, A. Kokalj, M. Lazzeri, L. Martin-Samos, N. Marzari, F. Mauri, R. Mazzarello, S. Paolini, A. Pasquarello, L. Paulatto, C. Sbraccia, S. Scandolo, G. Sclauzero, A. P. Seitsonen, A. Smogunov, P. Umari, R. M. Wentzcovitch, *J. Phys. Condens. Matter* **2009**, *21*, 395502.

[24] A. D. Becke, *J. Chem. Phys.* **1993**, *98*, 5648; C. Lee, W. Yang, R. G. Parr, *Phys. Rev. B* **1988**, *37*, 785.

[25] S. J. Clark, M. D. Segall, C. J. Pickard, P. J. Hasnip, M. I. J. Probert, K. Refson, M. C. Payne, *Z. Kristallogr.* **2005**, *220*, 567.